Surface analysis of cleaved single-crystalline $CaSi_2$ by Auger electron spectroscopy

Toshiyuki Hirano and Jun Fujiwara
National Research Institute for Metals, 1-2-1, Sengen, Tsukuba, Ibaraki 305, Japan
(Received 4 September 1990; revised manuscript received 26 November 1990)

The cleaved $CaSi_2$ (111) plane exhibited atomically smooth terraces with steps, and the secondary electron microscope (SEM) image showed a dark and bright contrast on the terrace. The Auger intensities showed a clear contrast corresponding to the SEM image contrast: The intensity of Si *LVV* was high in the dark region and low in the bright region, while the intensity of Ca *LMM* was reversed. The surface termination of the cleaved $CaSi_2$ (111) was quantitatively determined from the Auger-electron-spectroscopy point analysis such that the dark region was terminated in the Si bilayer and the bright region in the Ca monolayer. The results show that the cleavage occurs between the Ca monolayer and Si bilayer.

I. INTRODUCTION

$CaSi_2$ has received extensive attention as a new metal-semiconductor interfacial material in very large-scale integrated (VLSI) technology since an atomically smooth epitaxial film is grown on silicon wafers.[1,2] In the past, such an ideal interface on silicon was found only for $CoSi_2$ and $NiSi_2$.[3–8] The crystal structure of $CaSi_2$ shows layer-by-layer packing in which hexagonal Si bilayers alternate with hexagonal Ca monolayers along the [111] direction.[9] The basic structural features of the epitaxial $CaSi_2$ film are investigated by cross-sectional electron microscopy.[1,2] Theoretical and experimental studies of the electronic properties and structures have also been performed on the bulk polycrystals.[10–14] More detailed knowledge of the structures of this compound is critical for our understanding of the physical and chemical properties.

Recently, one of the authors reported the growth of a large single crystal of $CaSi_2$ by a floating-zone method and its electrical properties.[15] The single crystal of $CaSi_2$ exhibited a very smooth cleaved (111) surface just like mica. In this paper, we will present the results of surface analysis of the clean cleaved $CaSi_2$ (111) by Auger electron spectroscopy (AES). Our purpose in this study is to examine the termination of the cleaved (111) surface. The cleaved surface structure of $CaSi_2$ is of considerable scientific interest in view of the chemical bonding in this compound. Since $CaSi_2$ has a layered structure, the termination of the cleaved surface will serve to elucidate the chemical bonding. It is also of technological importance since the termination of the substrate surface strongly affects the growth of subsequent epitaxial layers. Such an effect has been studied for the metal overlayer growth on the transition-metal disilicides $CoSi_2$ (111), $FeSi_2$ (001), and $MoSi_2$ (001).[16,17] We will show, using surface-sensitive analysis AES, that cleavage occurs between the Ca monolayer and Si bilayer, resulting in the Ca monolayer termination and Si bilayer termination.

II. CRYSTAL STRUCTURE OF $CaSi_2$

$CaSi_2$ has a trigonal and rhombohedral structure with $a=10.42$ Å and $\alpha=21.5°$ and two molecules in the unit cell, as shown in Fig. 1(a). The fundamental crystal structure data[9] are listed in Table I. The stacking sequence along the [111] direction is an alternating repetition of hexagonal Ca monolayers and hexagonal Si bilayers, as shown in Fig. 1(b). There are 18 layers (6 Ca monolayers and 6 Si bilayers) in the entire stacking sequence. Two inequivalent Si atoms, Si(1) and Si(2), exist in the unit cell. Both Si atoms have a three Si first neighbors at 2.44–2.45 Å (slightly longer than the 2.35-Å bond length in pure silicon) in their neighboring Si layer. The major difference between Si(1) and Si(2) is a Ca atom coordination surrounding the Si atom as pointed out by Bisi *et al.*;[11] i.e., Si(1) has one Ca second neighbor at 3.06 Å while Si(2) does not. The interspacing of the Si bilayer,

TABLE I. Structural data of $CaSi_2$ (taken from Ref. 9). Bravais lattice: trigonal and rhombohedral; space group: $R3m$; lattice parameters: $a=10.42$ Å, $\alpha=21.5°$; atomic positions: Ca (0.083, 0.083, 0.083), Si(1) (0.185, 0.185, 0.185), Si(2) (0.352, 0.352, 0.352).

Atom	Neighbor	Coordination number	Distance (Å)
Ca	Si(2)	3	3.01
	Si(1)	3	3.03
	Si(1)	1	3.06
	Ca	6	3.86
Si(1)	Si(1)	3	2.44
	Ca	3	3.03
	Ca	1	3.06
	Si(1)	6	3.86
Si(2)	Si(2)	3	2.45
	Ca	3	3.01
	Ca	3	3.78
	Si(2)	6	3.86

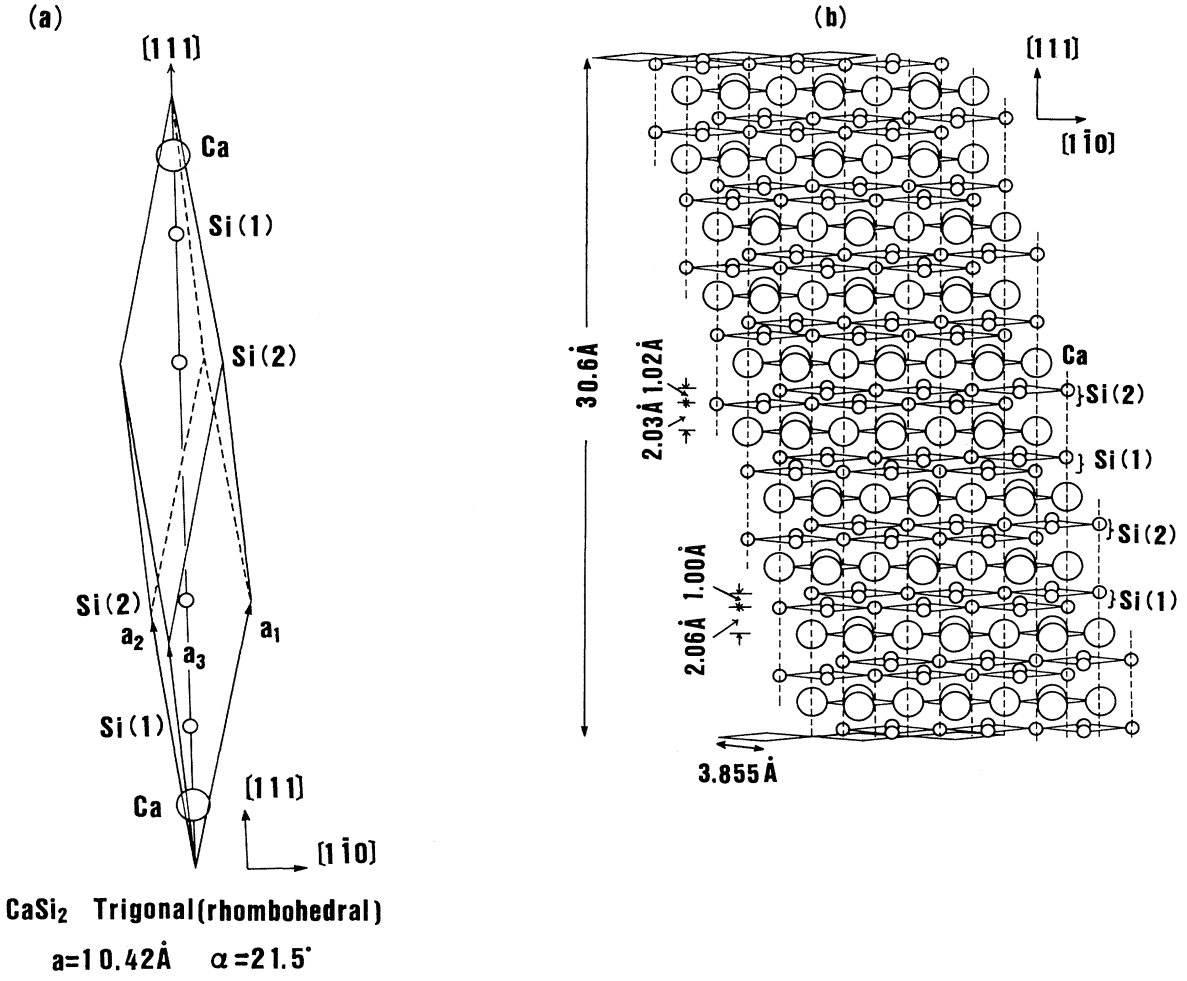

FIG. 1. (a) Unit cell of $CaSi_2$ and (b) the stacking sequence of atoms along the [111] direction.

1.00–1.02 Å, is considerably smaller than that between the Ca layer and Si layer, 2.03–2.06 Å.

III. EXPERIMENTS

Single-crystal growth of $CaSi_2$ was reported in a previous paper.[15] The crystals were grown in a flowing Ar atmosphere by a floating-zone method. The crystal structure was confirmed as a trigonal and rhombohedral structure by x-ray diffraction. The chemical composition of the crystals was also confirmed to be stoichiometric by electron-probe x-ray microanalysis. There were no detectable compositional distributions along the growth and radial directions in the as-grown crystals. The crystals were cut to give rectangular bars of $2\times2\times15$ mm^3 with 2×2 mm^2 faces perpendicular to the [111] direction. These specimens were notched to facilitate the cleavage in the Auger machine and then rinsed in acetone.

The Auger point analysis was carried out for the quantitative analysis of the cleaved surface with a scanning Auger microprobe (PHI SAM-660). An electron beam voltage of 5 keV with a beam current of 200 nA was used for the experiments. Auger electron spectra were recorded according to the $N(E)$ mode. The derivative spectra were calculated from these data. The beam spot size was 2.0 μm in diameter. The specimen was placed perpendicular to the axis of the cylindrical mirror analyzer (CMA), making the coaxial electron beam perpendicular to the specimen surface. The takeoff angle of Auger electron was 42° with respect to the specimen normal. The line-scanning Auger analysis was also carried out to examine the surface elemental distribution by the two-point method, i.e., by measuring the Auger peak height above the background. Once under vacuum, the specimens were cleaved *in situ* at a pressure of 3×10^{-10} Torr. Since $CaSi_2$ is metallic,[15] there were no surface-charge problems during the analysis: the electrical resistivity ranges between 56 and 63 $\mu\Omega$ cm at room temperature, depending on the crystal orientation.

IV. RESULTS

Cleavage occurred on the (111) plane, as described in a previous paper.[15] The cleaved surface exhibited smooth

terraces with steps, as shown in Fig. 2. Figure 2 is a micrograph of the cleaved surface by secondary electron microscopy (SEM) which is installed in the Auger machine. Each terrace looks like an atomically smooth surface and therefore there are no problems for the AES quantitative analysis due to the surface roughness. A striking feature in the SEM image is that a dark and bright contrast is observed on the terrace. Several factors are responsible for the SEM image contrast: (i) incident electron beam angle, (ii) chemical composition, (iii) surface roughness, and (iv) surface contamination.[18] We can neglect factors (i) and (iii) for the present smooth cleaved terrace. We can also neglect factor (iv) since the SEM observation was carried out under ultrahigh-vacuum conditions. In fact, the measured AES spectra show very low surface contamination, as will be described later. Consequently, we can consider that the presently observed contrast is due to factor (ii). The Auger analysis will show that this contrast reflects the topological difference in the surface chemical composition.

Figures 3(a) and 3(b) show the AES derivative spectra of the dark and bright regions, respectively. The cleaved surface is free from surface contamination such as carbon and oxygen. We see a large difference in the intensity ratio of Si *LVV* to Ca *LMM* between the dark and bright regions. In the dark region, the intensity of Si *LVV* is comparable with that of Ca *LMM*, while in the bright region, the former is considerably lower than the latter. The line-scanning Auger analysis has revealed that the SEM image contrast is due to the topological difference of the surface chemical composition. The Auger peak heights of Si *LVV* and Ca *LMM* were measured along points $A-M$ in Fig. 2., and the results are shown in Fig. 4. Points $A-M$ in Fig. 4 have one-to-one correspondence to the points given by the same symbols in Fig. 2. We clearly see the steplike changes of the Auger peak heights of Si *LVV* and Ca *LMM* on the terrace. The peak heights of Si *LVV* are high in the dark region and low in the bright region, while the peak height of Ca *LMM* is reversed. The fluctuation in the peak heights of both Si *LVV* and Ca *LMM* is very small within each terrace, and there is little difference in the peak heights between the terraces. At the steps, points $E-H$, both peak heights increase simultaneously due to the surface roughness. As far as we know, there are no reports of such a remarkable SEM image contrast corresponding to the changes of the Auger intensities for the homogeneous substance. Usually, SEM image contrast due to compositional distribution is observed for the heterogeneous substance, for example, the specimen surface segregated by heat treatment.[19]

Considering that the specimen is a homogeneous single crystal with layer-by-layer packing of the Ca monolayers and Si bilayers, we can expect that the SEM image con-

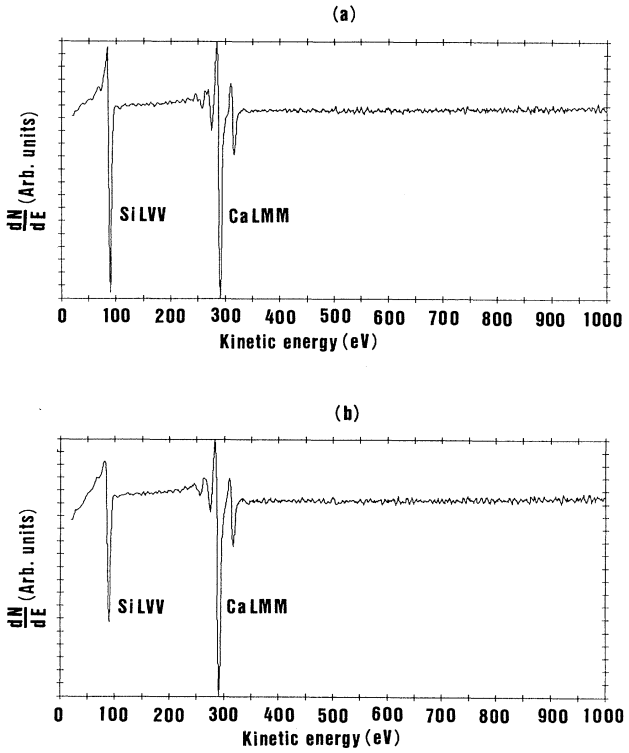

FIG. 3. Auger electron spectra of (a) the dark region and (b) the bright region of the cleaved $CaSi_2$ (111).

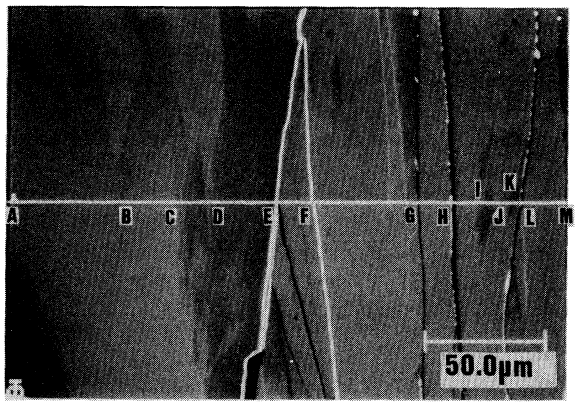

FIG. 2. SEM image of the cleaved (111) plane of $CaSi_2$.

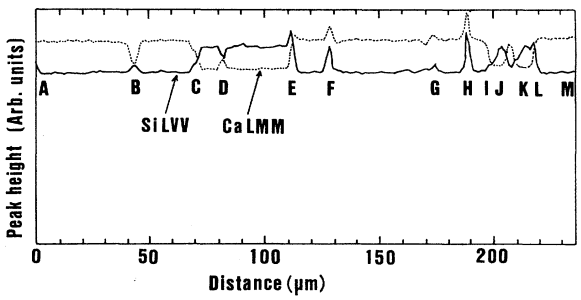

FIG. 4. Line-scanning AES analyses of Si *LVV* and Ca *LMM* of the cleaved $CaSi_2$ (111). The Auger peak heights were measured by the two-point method along points $A-M$ in Fig. 2.

TABLE II. Summary of the AES point analysis of the cleaved $CaSi_2$.

	Intensity (k counts/sec)		Intensity ratio
	$I_{Si\ LVV}$	$I_{Ca\ LMM}$	$I_{Si\ LVV}/I_{Ca\ LMM}$
Bright region	1410(±6)	2075(±18)	0.68(±0.02)
Dark region	2150(±13)	2170(±30)	0.99(±0.06)

trast is attributed to the surface termination of the cleaved surface; i.e., cleaving forms two kinds of surface termination, Ca-terminated and Si-terminated surfaces. The Auger point analysis was carried out in the dark and bright regions in order to confirm this expectation quantitatively. Table II summarizes the intensities of Si *LVV* and Ca *LMM*, and the intensity ratio of Si *LVV* to Ca *LMM* in both regions. These values are the averaged ones of the five points from the AES derivative spectra for each region. The intensity ratio of Si *LVV* to Ca *LMM*, $I_{Si\ LVV}/I_{Ca\ LMM}$, is 0.68 in the bright region and 0.99 in the dark region. We will determine the termination of the cleaved surface from these data in the following section.

V. DISCUSSION

$CaSi_2$ shows an atomically smooth cleaved surface parallel to the (111) plane, as shown in Fig. 2. From the layered structure, two possibilities of the cleavage can be considered, i.e., (i) between the Ca monolayer and Si bilayer, and (ii) between the Si bilayer. Then we can expect three different termination models, as shown in Fig. 5, i.e., (a) Ca monolayer termination, (b) Si bilayer termination, and (c) Si monolayer termination. It is probably impossible to distinguish the two inequivalent Si bilayers Si(1) and Si(2) since the difference between them is too small: the difference is the more than second-order Ca atom coordination around the Si atom, as mentioned in Sec. II. We will show that the Auger intensities correspond to the surface termination models of Figs. 5(a) and 5(b).

As Powell and Seah stated in their recent critical review,[20] it is practically unattractive to perform quantitative AES analysis from a first-principles equation. The simplest way of calculating the Auger electron intensity of the element i, I_{iWXY}, is to use the relative sensitivity factor S_i as follows:

$$I_{iWXY}=I_pS_in_iR\ , \tag{1}$$

where I_p is the primary electron beam current, n_i is the atomic concentration, and R is the surface roughness factor. In the case of layered compounds such as $CaSi_2$, n_i has an atomic-order depth distribution; i.e., it changes discretely for each crystal plane toward the interior of the specimen. Since AES is an extremely surface-sensitive analysis, the Auger electrons from the outermost surface atoms make the most significant contribution to the Auger intensity given by Eq. (1). In addition, the Auger electrons from the subsurface atoms are superimposed on them. Considering the attenuation length of the Auger electron, Eq. (1) is rewritten as

$$I_{iWXY}=I_pS_i\sum_j n_i(z_j)\exp(-z_j/\lambda_{iWXY}\cos\theta)\ , \tag{2}$$

where z_j is the distance of the jth crystal plane from the outermost surface, λ is the attenuation length, and θ is the takeoff angle of the Auger electron with respect to the specimen surface normal. In $CaSi_2$, $n_i(z_j)=5.83\times10^{-2}$ Å^2 for both the Ca layer and Si layer of the (111) planes, and $\theta=42°$. The attenuation lengths of Si *LVV* and Ca *LMM* are given empirically (in nm) by Seah and Dench for inorganic compounds:[21]

$$\lambda=2170aE^{-2}+0.72a^{3/2}E^{1/2}\ . \tag{3}$$

E is the kinetic energy of the Auger electron (in eV) and a is the monolayer thickness (in nm) given by

$$a^3=10^{21}A/\rho nN_a\ , \tag{4}$$

where N_a is Avogadro's number, ρ is the density (in g cm^{-3}), n is the number of molecules per unit cell, and A is the atomic weight. The attenuation lengths are summarized in Table III with their relative sensitivity factors.[22] Then the intensity ratio of $I_{Si\ LVV}$ to $I_{Ca\ LMM}$ is written by

$$\left[\frac{I_{Si\ LVV}}{I_{Ca\ LMM}}\right]=\left[\frac{S_{SI\ LVV}}{S_{Ca\ LMM}}\right]\left[\frac{\sum_j\exp(-z_j/\lambda_{Si\ LVV}\cos\theta)}{\sum_j\exp(-z_j/\lambda_{Ca\ LMM}\cos\theta)}\right]\ . \tag{5}$$

The calculated intensity ratios are strongly dependent on the termination models, as summarized in Table IV.

A comparison of Table III with Table IV reveals that the calculated $I_{Si\ LVV}/I_{Ca\ LMM}$ for model A agrees well with the measured value in the bright region within the

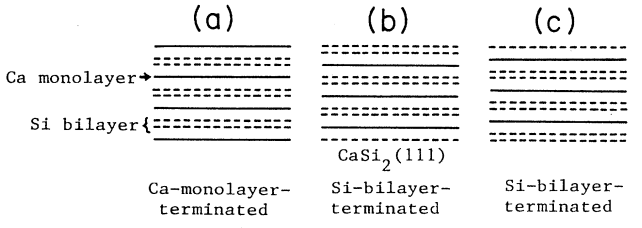

FIG. 5. Three possible surface termination models for the cleaved $CaSi_2$ (111). (a) Ca-monolayer-, (b) Si-bilayer-, and (c) Si-monolayer-terminated surfaces.

TABLE III. Summary of the parameters used for the quantitative AES point analysis.

	Relative sensitivity factor (Ref. 22) S_i	Attenuation length (Å) (Ref. 21) λ_i
Si *LVV*	0.28	10.9
Ca *LMM*	0.40	18.2

TABLE IV. Summary of the calculated AES intensity ratios based on the surface termination models in Fig. 5.

Termination model	$I_{Si\ LVV}/I_{Ca\ LMM}$
A Ca monolayer	0.68
B Si bilayer	1.11
C Si monolayer	0.88

accuracy of 1.4%. We can say that the bright region is terminated in the Ca monolayer. The measured $I_{Si\ LVV}/I_{Ca\ LMM}$ in the dark region, on the other hand, fell on the intermediate value between models B and C. Model B agrees with the measured value within the accuracy of 10.8% and model C does within the accuracy of 12.5%. Since the difference in the calculated $I_{Si\ LVV}/I_{Ca\ LMM}$ between models B and C is small, it is difficult to distinguish between the Si-monolayer-terminated and Si-bilayer-terminated surfaces. However, the above results on the bright region indicate that the cleavage occurs between the Ca monolayer and Si bilayer, leading to the formation of the Ca monolayer and Si bilayer on the surface, and therefore, we consider that the dark region is the Si-bilayer-terminated surface. Consequently, the surface structure of the cleaved $CaSi_2$ (111) can be schematically illustrated as Fig. 6. Cleavage yields smooth terraces consisting of the Ca-monolayer- and Si-bilayer-terminated surfaces accompanied with steps. The SEM image becomes bright on the Ca-monolayer-terminated surface, where the intensity of Ca *LMM* is high and it becomes dark on the Si-bilayer-terminated surface, where the intensity of Si *LVV* is high.

It is a reasonable conclusion that the cleavage occurs between the Ca layer and Si bilayer. First is the geometrical reason. The interspacing of the Si bilayer is considerably smaller than that between the Ca monolayer and Si bilayer, as mentioned in Sec. II. Second is the chemical bond in this compound. Bisi *et al.* recently reported a combined theoretical and experimental investigation of the chemical bond and electronic states in calcium silicides (Ca_2Si, CaSi, and $CaSi_2$).[11] They showed evidence of an extensive interaction between the Si *s-p* and Ca *s-p-d* states. This interaction is a characteristic feature of the chemical bond of $CaSi_2$. Very recently, Fahy and Hamann also calculated the electronic and structural properties of $CaSi_2$ and found a strong hybridization of Ca *d* states with Si *p* states.[14] However, they showed that the Si-Si bond charge is relatively unchanged compared with pure silicon and there is no sign of a clear bond

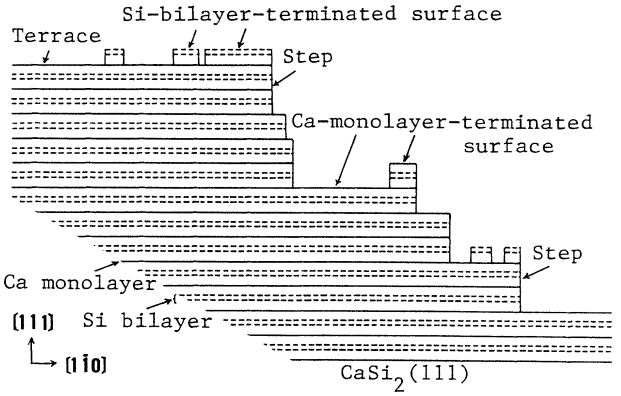

FIG. 6. Schematic illustration of the surface structure of the cleaved $CaSi_2$.

charge between the Ca and Si atoms because of the very small effect of the Ca coordination number with Si on the structure energy. Their calculation seems to be reasonable since the Si-Si bond length is similar to that in pure silicon. Their results indicate that the Ca-Si bonding is weaker than the Si-Si bonding in $CaSi_2$ and therefore support the present results that the cleavage occurs between the Ca monolayer and Si bilayer.

VI. CONCLUSIONS

We presented an AES analysis of the clean cleaved $CaSi_2$ (111) surface. The cleaved surface exhibited atomically smooth terraces with steps and the SEM image of the surface showed a dark and bright contrast on the terrace. The Auger intensities of Si *LVV* and Ca *LMM* showed a clear contrast on the terrace, corresponding to the SEM image contrast. The intensity of Si *LVV* was high in the dark region and low in the bright region, while the intensity of Ca *LMM* was reversed. We could quantitatively determine the surface termination of the cleaved $CaSi_2$ (111) such that the dark region was terminated in the Si bilayer and the bright region in the Ca monolayer. The results indicate that the cleavage occurs between the Ca monolayer and Si bilayer.

ACKNOWLEDGMENTS

We would like to acknowledge Dr. K. Ogawa for his suggestion of this study and critical reading of this manuscript. We also would like to acknowledge Dr. K. Yoshihara and Dr. Y. Yamauchi for their helpful discussions on the results of the AES analysis.

[1]J. F. Morar and M. Wittmer, Phys. Rev. B **37**, 2618 (1988).
[2]J. F. Morar and M. Wittmer, J. Vac. Sci. Technol. **A6**, 1340 (1988).
[3]S. Saitoh, H. Ishiwara, and S. Furukawa, Appl. Phys. Lett. **37**, 203 (1980).
[4]J. M. Gibson, J. C. Bean, J. M. Poate, and R. T. Tung, Appl. Phys. Lett. **37**, 643 (1980).
[5]S. Saitoh, H. Ishiwara, T. Asano, and S. Furukawa, Jpn. J. Appl. Phys. **20**, 1649 (1981).
[6]K. C. R. Chiu, J. M. Poate, J. E. Rowe, T. T. Sheng, and A. G. Cullis, Appl. Phys. Lett. **38**, 988 (1981).
[7]R. T. Tung, J. M. Gibson, J. C. Bean, J. M. Poate, and D. C.

Jacobson, Appl. Phys. Lett. **40**, 684 (1982).
[8]R. T. Tung, J. M. Gibson, and J. M. Poate, Phys. Rev. Lett. **50**, 429 (1983).
[9]P. Villars and L. D. Calvert, *Pearson's Handbook of Crystallographic Data for Intermetallic Phases* (American Society for Metals, Metals Park, Ohio, 1985).
[10]M. Sancrotti, I. Abbati, L. Calliari, F. Marchetti, O. Bisi, A. Iandelli, G. L. Olcese, and A. Palenzona, Phys. Rev. B **37**, 4805 (1988).
[11]O. Bisi, L. Braicovich, C. Carbone, I. Lindau, A. Iandelli, G. L. Olcese, and A. Palenzona, Phys. Rev. B **40**, 10 194 (1989).
[12]C. Chemelli, M. Sancrotti, L. Braicovich, F. Ciccacci, O. Bisi, A. Iandelli, G. L. Olcese, and A. Palenzona, Phys. Rev. B **40**, 10 210 (1989).
[13]L. Calliari, F. Marchetti, M. Sancrotti, O. Bisi, A. Iandelli, G. L. Olcese, and A. Palenzona, Phys. Rev. B **41**, 7569 (1990).
[14]S. Fahy and D. R. Hamann, Phys. Rev. B **41**, 7587 (1990).
[15]Toshiyuki Hirano, J. Less-Common Met. (to be published).
[16]J. P. Sullivan, Toshiyuki Hirano, T. Komeda, H. M. Meyer III, B. M. Trafas, G. D. Waddill, and J. H. Weaver, Appl. Phys. Lett. **56**, 671 (1990).
[17]T. Komeda, Toshiyuki Hirano, G. D. Waddill, Steven G. Anderson, J. P. Sullivan, and J. H. Weaver, Phys. Rev. B **41**, 8345 (1990).
[18]D. E. Newbury, in *Practical Scanning Electron Microspectroscopy,* edited by J. I. Goldstein and H. Yakowitz (Plenum, New York, 1975), p. 95.
[19]R. R. Olson, P. W. Palmberg, C. T. Hovland, and T. E. Brady, in *Practical Surface Analysis by Auger and X-Ray Photoelectron Spectroscopy,* edited by D. Briggs and M. P. Seah (Wiley, Chichester, 1983), p. 217.
[20]C. J. Powell and M. P. Seah, J. Vac. Sci. Technol. **A8**, 735 (1990).
[21]M. P. Seah and W. A. Dench, Surf. Interface Anal. **1**, 2 (1979).
[22]L. E. Davis, N. C. MacDonald, P. W. Palmberg, R. E. Riach, and R. E. Weber, *Handbook of Auger Electron Spectroscopy* (Physical Electronics Industries, Minnesota, 1976).

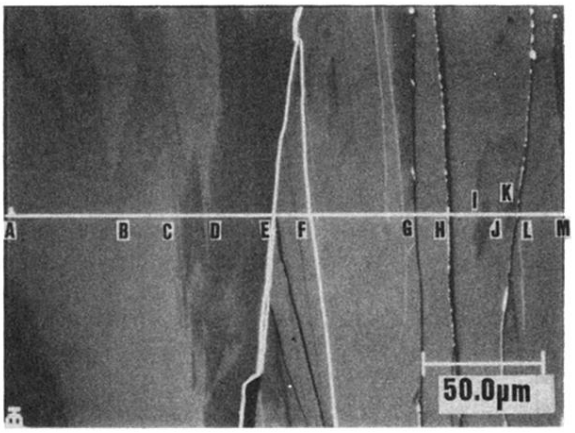

FIG. 2. SEM image of the cleaved (111) plane of $CaSi_2$.